Bioactive Materials 5 (2020) 142–152

Contents lists available at ScienceDirect

Bioactive Materials

journal homepage: http://www.keaipublishing.com/biomat

Recruitment of endogenous progenitor cells by erythropoietin loaded particles for in situ cartilage regeneration

Amirhossein Hakamivala[a], Shuxin li[a], Kayti Robinson[b], YiHui Huang[a], Shuai Yu[a], Baohong Yuan[a], Joseph Borrelli Jr.[a], Liping Tang[a,*]

[a] Bioengineering Department, University of Texas Southwestern Medical Center, The University of Texas at Arlington, Arlington, TX, 76019, USA
[b] Department of Biology, The University of Texas at Arlington, Arlington, TX, 76019, USA

ARTICLE INFO

Keywords:
Hyaluronic acid microscaffolds
Erythropoietin
Progenitor cells recruitment
Chondrogenesis
Cartilage injury

ABSTRACT

Cartilage injury affects millions of people throughout the world, and at this time there is no cure. While transplantation of stem cells has shown some success in the treatment of injured cartilage, such treatment is limited by limited cell sources and safety concerns. To overcome these drawbacks, a microscaffolds system was developed capable of targeting, reducing the inflammatory response and recruiting endogenous progenitor cells to cartilage-defect. Erythropoietin (EPO)-loaded-hyaluronic acid (HA) microscaffolds (HA + EPO) were fabricated and characterized. HA-microscaffolds showed good cell-compatibility and could target chondrocytes via CD44 receptors. HA + EPO was designed to slowly release EPO while recruiting progenitor cells. Finally, the ability of HA + EPO to repair cartilage-defects was assessed using a rabbit model of full-thickness cartilage-defect. Our results showed that the intra-articular administration of EPO, HA, and EPO + HA reduced the number of inflammatory cells inside the synovial-fluid, while EPO + HA had the greatest anti-inflammatory effects. Furthermore, among all groups, EPO + HA achieved the greatest progenitor cell recruitment and subsequent chondrogenesis. The results of this work support that, by targeting and localizing the release of growth-factors, HA + EPO can reduce inflammatory responses and promote progenitor cells responses. This new platform represents an alternative treatment to stem-cell transplantation for the treatment of cartilage injury.

1. Introduction

Post-traumatic osteoarthritis (PTOA) is a type of osteoarthritis that develops after joint injury and is most prevalent in the ankles, knees and hips [1]. It is estimated that more than 6 million people alone in the US suffer from PTOA which accounted for annual healthcare expenditures of approximately 3 billion dollars (US) in 2013 [2]. All indications are that PTOA will pose an even more significant challenge in the coming years as the US and world's population continues to age and people remain active and more likely to injure their joints. An effective, safe, less invasive and cost-effective means of treating PTOA is therefore much needed. The current standard therapy for PTOA includes muscle-strengthening exercise, weight loss, the use of anti-inflammatory drugs, intra-articular injections and in many cases surgical intervention [3]. Unfortunately, none of these options alter the natural history of the disease nor restore the full function of these injured cartilages. In recent years, substantial progress has been made in the area of stem cells and tissue engineering for regeneration of cartilage tissues. Specifically, it is well established that mesenchymal stem cells (MSCs) can be differentiated into chondrocytes to form cartilage-like tissue in culture [4,5]. Furthermore, recent studies have indicated that isolation, purification and injection of progenitor cells into the diathrodial joints may improve cartilage regeneration after the onset of osteoarthritis, by reducing localized inflammatory responses in mice [6,7]. However, administration of MSCs for cartilage regeneration has limited applications due to the costly and time-consuming processes of isolating, expansion and culture of autologous MSCs. To overcome these limitations, recent studies utilized endogenous synovial progenitor/stem cells for tissue regeneration in cartilage defects by homing resident progenitor cells to the site of injury [8,9]. In addition, several recent reports have documented the presence of the synovial progenitor/stem cells in the synovial fluid/membrane and the numbers of progenitor cells increased with the severity of OA. Interestingly, chemoattractant releasing scaffolds have been used as a strategy to cue these progenitor cells to the site of the injury for inducing chondrogenesis. For example, acellular cartilage matrix conjugated with a bone marrow homing peptide has

Peer review under responsibility of KeAi Communications Co., Ltd.
* Corresponding author. Bioengineering Department, the University of Texas at Arlington, P.O. Box 19138, Arlington, TX, 76019-0138, USA.
E-mail address: ltang@uta.edu (L. Tang).

https://doi.org/10.1016/j.bioactmat.2020.01.007
Received 6 August 2019; Received in revised form 12 November 2019; Accepted 12 January 2020

been employed to repair full-thickness cartilage defect in a rabbit model by triggering endogenous progenitor/stem cell recruitment [8]. To elicit sustained endogenous progenitor cell recruitment, micro/nanoparticles have been used as microscaffolds to support cell growth and differentiation by the localized release of growth factors at the site of injury [10].

Hyaluronic acid (HA) based particles are a good microscaffold candidate for cartilage tissue engineering. First, HA, is a naturally occurring polysaccharide, and has been used in many tissue engineering applications [11]. Second, HA is the main component of synovial fluids and cartilage matrix and can be degraded in the presence of hyaluronidase (HAase) existing in synovial fluid [12]. Third, it is well established that HA particles have a high affinity for cells with CD44 receptors [13]. Since the expression of CD44 in articular cartilage tissue is closely correlated with the severity of OA [14,15], it is likely that HA particles can accumulate on the surface of injured cartilage by targeting its CD44 receptors. Finally, HA microscaffolds have been developed as an effective carrier for targeted delivery of BMP-2 *in vitro* to promote cartilage repair and regeneration [16]. However, to the best of our knowledge, microscaffolds systems have not been explored for their ability to induce endogenous progenitor cell-mediated cartilage repair.

This report summarizes a study which was aimed at developing a new technology for triggering intrinsic cartilage regeneration by provoking endogenous progenitor cell responses. Briefly, HA microscaffolds were fabricated to targeted $CD44^+$ chondrocytes. Some of these microscaffolds were loaded with erythropoietin (EPO). EPO is an FDA approved growth factor with the ability to modulate/progenitor/stem cell responses including proliferation and differentiation [17]. Localized released of EPO has been shown to promote endogenous progenitor cell recruitment and osteogenic differentiation at the site of bone defect *in vivo* [18]. Using both *in vitro and ex vivo* models, we assessed the ability of HA microscaffolds to target activated human chondrocytes and OA cartilage tissues. Finally, using rabbit microfracture defect model [19], we investigated the ability of HA microscaffolds, EPO, HA microscaffolds + EPO to promote endogenous progenitor cell responses and chondrogenesis at the site of injured cartilage.

2. Materials and methods

2.1. Materials

Hyaluronic acid sodium salt (HA) (700 KDa) was purchased from LifeCore Biomedical (Chaska, MN). 1-heptanol (98%) and NaCl were obtained from Sigma-Aldrich (St. Louis, MO). Dioctyl sulfosuccinate sodium salt (AOT, 96%), divinyl sulfone (DVS, 98%) and, 2,2,4-Trimethylpentane (isooctane, 99%) were purchased from Fisher Scientific (Hampton, NH). CF488A and CF647A amine dye were supplied from Biotium, Inc. (Fremont, CA). *N*-Hydroxysuccinimide (NHS) was purchased from Thermo Scientific (Rockford, IL). Collagenase type 2 was purchased from Worthington Biochemical (Lakewood, NJ). Erythropoietin (EPO) was purchased from Amgen Inc. (Thousand Oak, CA). CD29 (FITC-conjugated anti-human integrin β1 monoclonal antibody (MAB1951F-100) and CD90 (Alexa Fluor 594-conjugated anti-rat/mouse Thy1.1, Ox-7) were purchased from Millipore (Darmstadt, Germany) and BioLegend (San Diego, CA), respectively.

2.2. Cell isolation and culture

Human chondrocyte was isolated from discarded human OA tissues (N = 4) during arthroscopic surgery without patients' identity by following the published procedure [13]. The isolated cells were cultured with a concentration of 104 cells/ml in Dulbecco's Modified Eagle's medium (DMEM) (Sigma-Aldrich, St. Louis, MO) supplemented with 10% heat-inactivated fetal bovine serum (FBS) (Atlanta Biologicals, Atlanta, GA) and 1% penicillin/streptomycin (Gibco, Waltham, MA). Human bone marrow-derived mesenchymal stem cells (PCS-500-012) (ATCC, Manassas, VA) were cultured in mesenchymal stem cell basal medium (PCS-500-030) (ATCC, Manassas, VA) supplemented with 7% heat-inactivated FBS, 2.4 mM recombinant insulin-like growth factor-1, 5 ng/ml recombinant fibroblast growth factor-beta, 2.4 mM L-Alanyl-L-Glutamine (all from ATCC, Manassas, VA) and 1% penicillin/streptomycin. Bone marrow MSCs were used in this study to simulate progenitor cell responses following cartilage injury since microfracture procedure was used to create the cartilage defect and such a procedure can create an opening for the immigration of bone marrow MSCs from bone marrow.

2.3. HA microscaffold production and characterization

HA microscaffolds were prepared as described in a recent publication [20]. To enhance visualization of HA microscaffolds, some HA microscaffolds were labeled with fluorescent dyes (CF488A and CF647A amine dye) as described previously [21]. Morphology and microstructure of the HA microscaffolds were analyzed using Leica DMi8 Fluorescence microscope (Leica, Wetzlar, Germany) and scanning electron microscopy (FE-SEM, S-4800 316 Hitachi, operating at 5 kV). The size of microscaffolds was determined using ImageJ software (US National Institutes of Health). The cytotoxicity of HA microscaffolds was assessed using primary human chondrocytes isolated from normal human articular cartilage (from PromoCell, Heidelberg, Germany) and Alamar Blue assay (Bio-Rad, Hercules, CA, USA), according to the manufacturer's instructions [22]. Briefly, Human chondrocytes were seeded at a concentration of 5000 cells/well in 100 µl of complete medium in a 96-well plate and then cultured for 24 h. Different concentrations of HA micro-scaffolds (0–2 mg/ml in complete medium) were added to the cells and incubated for another 24 h. The cell viability was determined by adding 10 µl of Alamar Blue to each well following incubation at 37 °C for 4 h. The well plate was then read at an excitation wavelength of 560 nm and an emission wavelength of 610 nm in an Infinite M200 microplate reader (Tecan, San Jose, CA).

EPO loaded HA microscaffolds was prepared by mixing dried HA microscaffolds and EPO according to a previous report [16]. To determine loading capacity, EPO was labeled with FITC follow manufacturer's protocol [21]. Then the loading capacity was calculated based on the following equation: $\frac{EPO_{Intial} - EPO_{Supernatant}}{Mass\ of\ dried\ HA\ microscaffold}$ where $EPO_{Initial}$ and $EPO_{Supernatant}$ are mass of initial and not absorbed EPO, respectively, which were measured using the microplate reader and calculated based on the standard curve of FITC-Labeled-EPO. To determine EPO release, FITC-Labeled-EPO loaded HA microscaffolds were suspended in 0.5 ml of PBS (pH = 7). At various time points, the supernatants were collected and the released media were replenished with an, and amount of the fresh one. The amounts of released EPO were measured based on the fluorescence intensity of FITC-Labeled-EPO. The cumulative release was defined as the total amount of released EPO at a predetermined time relative to the initial loading amount. To test the bioactivity of the released EPO, a transwell migration assay was performed as described earlier [18,23]. Briefly, Transwell membranes with 8 µm pores (PET membrane) were coated on both sides with 10 µg/ml fibronectin (Sigma-Aldrich, St. Louis, MO) for 2 h at room temperature and rinsed once with PBS. Then, 670 µl of released EPO (fresh EPO as control) were placed in the lower chamber and 100 µl of 12 h serum-starved MSCs (10^6 cells/mL) were added to the top of the chamber. After incubation at 37 °C for 12 h, the non-migrated cells were removed with a cotton swab, and the migratory cells were fixed in 99% methanol and stained with Giemsa solution. The cell images were taken using an inverted phase contrast microscope at 10X and the number of migrated cells per membrane was counted using ImageJ software. The migration ability of MSCs toward the released EPO from microscaffolds was assessed compared to the free EPO.

2.4. Cell and tissue targeting property of HA microscaffolds

Different numbers of human chondrocytes (1, 2, 4 and 8 × 10^4) were incubated with CF647-HA microscaffolds (final concentration of 0.1 mg/mL in complete DMEM) for 15 min. They were centrifuged and then washed with fresh media 3X; the extent of scaffold binding to chondrocytes was assessed by measuring cell-associated fluorescent intensities using a microplate fluorometer. The extent of CD44 expression on different numbers of human chondrocytes was also measured using FITC-conjugated CD44 antibody (HCAM (IM7), sc-18849) Santa Cruz Biotechnology, Inc. (Dallas, Texas) by following manufacturer's instructions.

The ability of HA microscaffolds to target human cartilage tissue was also assessed *ex vivo* using discarded human articular cartilage tissue (N = 6) isolated during total knee replacement surgery without any patients' identification. The tissues were first incubated with different concentrations (0.02, 0.1 and 0.5 mg/mL) of CF647 conjugated-HA microscaffolds for varying periods (30, 60, 90, 120 and 180 min). After an extensive wash with complete media to remove unbounded microscaffolds, the tissues were then imaged using a Kodak *in vivo* FX Pro imaging system (Carestream Health Inc., New Haven, CT). Furthermore, to determine the role of CD44 in mediating HA microscaffolds accumulation, OA cartilage tissues were immersed in complete medium with or without CD44 HCAM (IM7) blocking antibody (final concentration 10 μg/ml) for 1 h. CF647-HA microscaffolds (final concentration of 100 μg/ml) was then added into each well and incubated at 37 °C for 30 min. The ability of HA microscaffolds to target CD44 blocked cartilage and its control was quantified using a Kodak *in vivo* imaging system. The collected images were processed according to our previous publication [24]. Data was plotted in terms of the mean intensity of Region of Interest.

2.5. Rabbit microfracture defect model

All animals were treated according to the standard guidelines approved by Animal Care and Use Committee (IACUC) at the University of Texas at Arlington in accordance with the Animal Welfare Act and Guide for the Care and Use of Laboratory Animals. New Zealand White Rabbits 3–6 months old weighing between 1.9 and 2.8 kg were randomly divided into 4 groups - saline, EPO alone, HA microscaffolds alone (abbreviated as HA) and EPO loaded HA microscaffolds (abbreviated as HA + EPO) (N = 4/group/time point) for 2 different time points (12 and 26 weeks). The animals were first undergone microfracture procedure [25,26]. Under general anesthesia (ketamine + xylazine injection and isoflurane inhalation), with the New Zealand White Rabbits in a prone position, the primary contact region of the medial femoral condyle was approached at an angle of 135° of flexion. A full-thickness cartilage defects (~3 mm) were created in the weight-bearing area of the medial femoral condyle with a dermal biopsy punch and manual debridement to expose the subchondral bone plate. Each specimen then was undergone microfracture. Microfracture holes were created within each full-thickness chondral defect using a 0.9-mm Kirschner wire tapped into the subchondral bone (~3 mm) until bleeding from the hole is apparent. By doing this, the subchondral bone was perforated to generate a blood clot within the defect. Once the defect was filled with different groups of HA microscaffolds, the patella were reduced; the joint capsule were closed with interrupted sutures. At the end of the procedure, 20 μL of different treatments (saline, EPO, HA, or HA + EPO) were implanted on top of the articular cartilage defects. The animals were allowed to move freely within their cages after surgery. After the predetermined time points, animals were sacrificed. The knee joints and synovial fluids were then recovered for the following analyses.

2.6. Analysis of synovial inflammatory cells

To quantify the numbers of inflammatory cells in synovial fluid, synovial fluid of the rabbits was aspirated after injection of 1 ml of normal saline solution into the joint space. The synovial fluid cells were spun down on glass slides using a cytospin (Cytospin 2, Thermo Shandon, Cheshire, England). The number of inflammatory cells was then determined using a immunocytochemistry technique and CD11b (M1/70; BioLegend, San Diego, CA) as described earlier [27].

2.7. Micro-computed tomography assessment

Micro-computed tomography assessment of cartilage/bone microarchitecture was carried out on some rabbit joints using a High throughput *in vivo* SkyScan micro-CT scanner (Bruker, Billerica, MA) with an exposure time of 640 ms/frame and the X-ray power at 39 W during an 18 min scan. 499 images were obtained at a rotation step of 0.72°. The scans were then reconstructed and analyzed using CTVox and CTAn software (Bruker, Billerica, MA). To avoid selecting the wrong defect areas, we decide to evaluate the whole joint and the bone volume fraction (BVF), which is defined as bone volume divided by tissue volume (BV/TV), for all of the samples [8,28].

2.8. Assessment of chondrogenesis and cartilage regeneration

Some tissue samples were fixed in 4% w/v buffered paraformaldehyde, decalcified, embedded in paraffin wax and then sectioned with an approximate thickness of 6 μm using a manual rotary microtome (Leica, Buffalo Grove, IL) by following published procedures [29,30]. The sections were subsequently stained with hematoxylin and eosin (H&E), Safranin O and Toluidine blue staining [31], followed by imaging via an inverted light microscope (Leica TCS SP8 SMD, Leica, Buffalo Grove, IL). The extent of cartilage repair was then evaluated using the Pineda scoring system (Table 1 supplementary) [32]. All the samples were presented and examined by two observers in a blinded and random order. Furthermore, Toluidine blue was quantified and reported as the optical density of the images went through deconvolution process in ImageJ [33].

The 12-weeks cartilage samples were assessed for progenitor cell recruitment to the site of injury utilizing immunohistochemistry. It has been documented that synovial stem cells possess dual markers of CD29 and CD90 [34–36]. Briefly, after antigen retrieval, the tissue sections were blocked with 10% goat serum for 30 mines and then followed by overnight incubation with CD29 (FITC-conjugated anti-human integrin β1 monoclonal antibody and at 4 °C. All the sections images were taken using a confocal laser scanning microscopy and analyzed by LAS X software (Leica, Buffalo Grove, IL). The number of CD29 and CD90 double-positive cells per mm^2 was determined by ImageJ software.

Collagen II production is well established to be a chondrogenic marker [5,37]. To detect Collagen II secretion in the cartilage, some of the 12- and 26-weeks tissue sections were stained with antibodies to Collagen II (M2139, sc-52658, Santa Cruz Biotechnology, Dallas, Texas), goat anti-mouse HRP secondary antibody (IgG H&L ab6789, Abcam) and finally diaminobenzidine was used as a chromogen as described earlier [38]. Collagen II was quantified as the percentage of positively stained areas versus the whole as previously established [39].

2.9. Statistical analysis

Scoring of histological staining of cartilage tissues are presented as medians ± interquartile range and analyzed with Mann-Whitney test. All other data are expressed as mean ± standard deviation. An independent student t-test was used for the two independent groups while one-way analysis of variance (ANOVA) was utilized for multi-group comparison. An F test was used to examine the equality of the variance. All statistical analyses were performed using SPSS 16 and XLSTAT. A p-

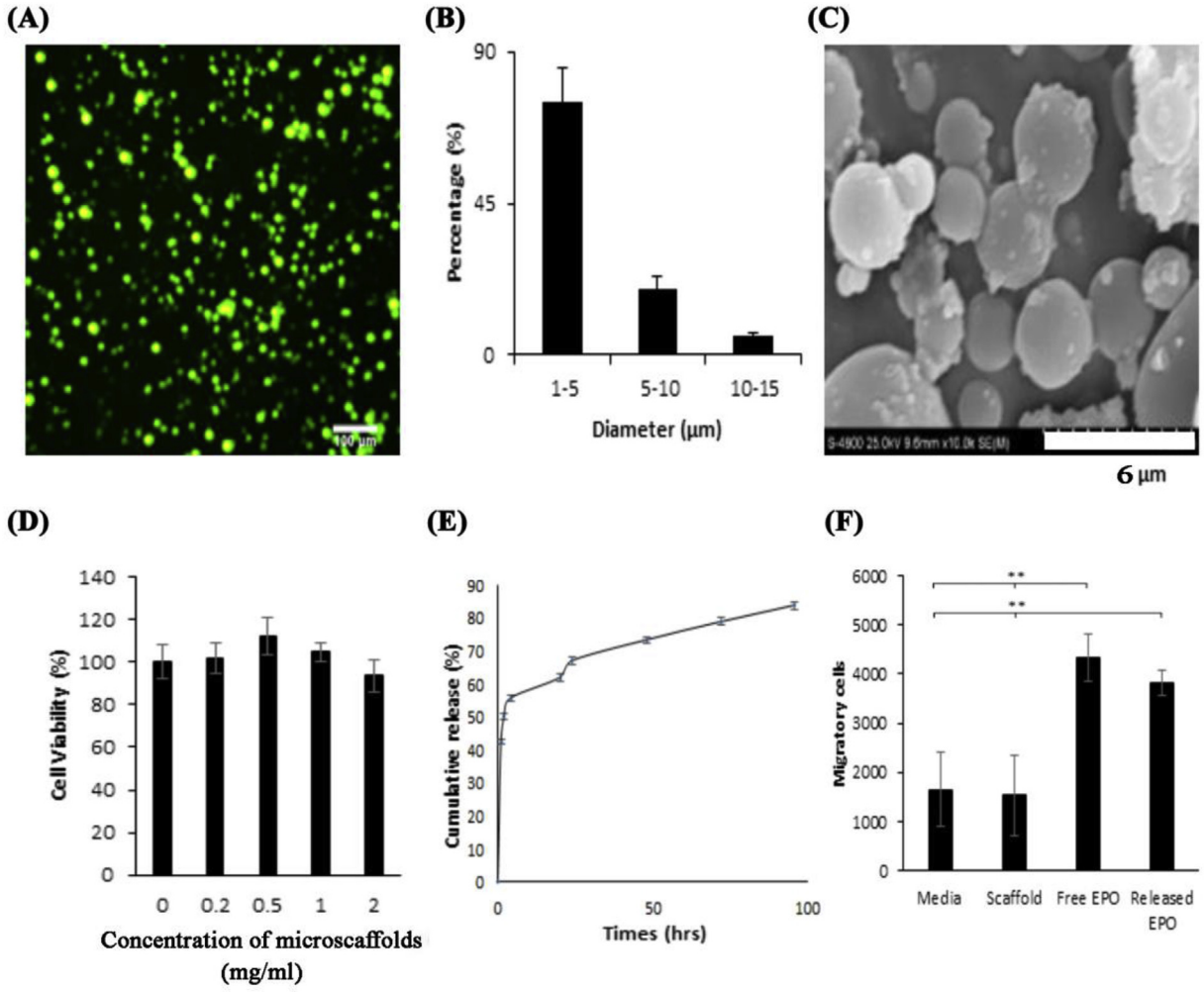

Fig. 1. Physical and biological characterization of HA microscaffolds loaded with EPO. (A) Fluorescence imaging (100x) of the FITC-conjugated microscaffolds; (B) size distribution calculated using ImageJ. (C) A representative SEM image of the microscaffolds; (D) In vitro cytotoxicity of HA microscaffolds using primary human chondrocytes and Alamar Blue assay. (Mean ± SD; n = 3; p = 0.197) (E) EPO release profile from HA microscaffolds (F) Recruitment of the human MSCs toward various groups (control, HA microscaffolds [labeled as "scaffold"], free EPO, or EPO released from scaffolds [labeled as "Released EPO"]) using Transwell migration assay. (Mean ± SD; n = 3; **p < 0.01).

value < 0.01 and 0.05 was considered statistically significant.

3. Results and discussions

3.1. Characterizations of HA microscaffolds and its EPO release property

The spherical morphology of FITC-labeled HA microscaffolds can be seen under a fluorescence microscope (Fig. 1A). The size distribution of HA microscaffolds was determined to be 1–15 µm with an average size of 4.2 µm (Fig. 1B). SEM images further confirmed the spherical shape of HA microscaffolds with a slight reduction in particle sizes (Fig. 1C) due to the sample dehydration during preparation for SEM. Our observations support that HA microscaffolds have good cell compatibility based on the viability of human chondrocytes that was unchanged in the presence of increasing concentrations (up to 2.0 mg/ml without statistical significance) of HA microscaffolds (Fig. 1D) The > 100% of cell viability might be attributed to the proliferative effect of HA microscaffold on chondrocytes.

To assess the ability of HA microscaffolds to release EPO, FITC-labeled-EPO was loaded into microscaffolds. The loading capacity was found to be 17.6 µg/mg. The ability of HA microscaffolds to release EPO was then evaluated. The release profile showed a fast release of EPO (~55%) during the first 4 h (Fig. 1E). This burst release may help to create a cytokine gradient that has been shown to be essential for cell recruitment [40]. The EPO release rate slowed down after 24 h with ~10% of the remaining EPO release per day. The EPO release rate from the HA scaffolds can be further delayed via chemical conjugation of the EPO to the HA microscaffolds. The slow release of EPO may create a EPO gradient important for achieving continuous recruitment of progenitor cells.

Since EPO is able to trigger the recruitment of MSCs [18] and is stable in a physiological condition, the bioactivity of released EPO was determined based on its ability to promote migration of progenitor cells (Fig. 1F). Our results show that HA microscaffolds by themselves have no MSCs recruitment activities, while released EPO can trigger MSCs recruitment. These results confirmed the bioactivity of released EPO and supported the potential for using EPO-loaded HA microscaffolds to promote MSCs recruitment into the site of injured cartilage. In fact, EPO has been shown to trigger the migration and proliferation of bone marrow derived MSCs and it has also been shown to promote chondrogenesis and chondrocyte proliferation [41].

3.2. The ability of HA microscaffolds to target chondrocytes and injured cartilage

The ability of HA microscaffolds to target chondrocytes through

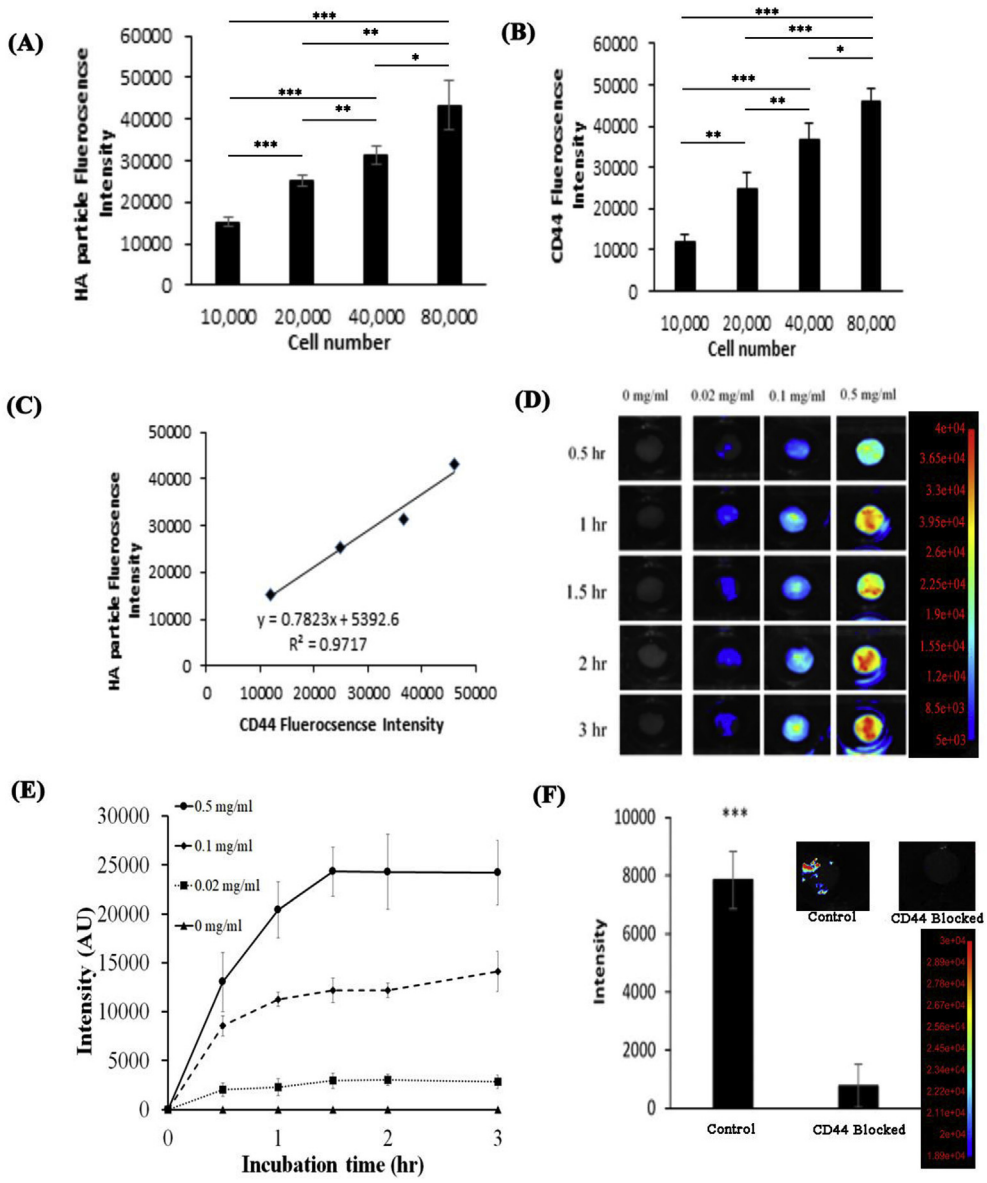

Fig. 2. *In vitro* characterization of HA microscaffolds. (A) The fluorescent intensity of FITC-conjugated HA microscaffolds associated with different numbers of human chondrocytes. (B) The fluorescent intensity of CD44 receptor associated with different numbers of human chondrocytes. (C) There was a good linear relationship between the amount of HA microscaffolds and the extent of CD44 receptor expression with an R^2 of 0.97. (D) Time and dose-dependent fluorescent images of osteoarthritic human tissue incubated with different concentrations of HA microscaffolds (0.02, 0.1 and 0.5 mg/ml). (n = 6) (E) The fluorescent intensities of all tissue incubated with different concentrations of HA microscaffolds for different periods of time (up to 180 min) were calculated and compared. (n = 6). (F) The fluorescent intensity associated to HA microscaffolds incubated with OA human explant tissue pre-treated with CD44 blocking antibody or control. (Mean ± SD; n = 3; *p < 0.5, **p < 0.01 and ***p < 0.001).

CD44 receptor was assessed using human cartilage cells and osteoarthritic tissue explants. We found that HA microscaffolds have good affinity for cartilage cells. In fact, the amount of cell-associated HA microscaffolds and the extent of CD44 expression increased with the increasing number of activated cells (Fig. 2A and B). Further analyses revealed a linear relationship (R^2 = 0.97) between the amount of HA microscaffolds and the extent of CD44 receptor expression (Fig. 2C). These results lend strong support that HA microscaffolds target chondrocytes via their CD44 receptors.

Further study was carried out to evaluate HA microscaffolds' capability of targeting injured human cartilage explants. Specifically, human OA tissues were incubated with different concentrations of HA microscaffolds for different periods of time. The accumulation of HA microscaffolds on different areas of OA tissues was then quantified using the Kodak *in vivo* imaging system. The images revealed that HA microscaffolds accumulation on OA tissues was both time and microscaffolds concentration dependent (Fig. 2D). By quantifying and comparing the tissue associated microscaffolds' fluorescent intensities (previously reported [24]), we found that, even at low concentrations, HA microscaffolds could target and accumulate on the surface of the OA tissue (Fig. 2E). The peak of the targeting efficiency occurred within 90 min of incubation and the accumulation of HA microscaffolds on tissue increased with increased concentrations of HA microscaffolds (Fig. 2E). We then investigated the role of CD44 on the HA microscaffold:OA tissue interaction using CD44 blocking antibody. Interestingly, our results show that the blockage of CD44 receptors significantly reduced the accumulation of the HA microscaffolds on OA tissue by a factor of 8 (Fig. 2F). Our results show the importance of CD44 receptor in mediating HA microscaffold-accumulation on injured cartilage tissue, and these findings were confirmed in a previous report [42]. Although there are insufficient results to exclude the participation of other receptor(s) in such reactions, these findings support our hypothesis that HA microscaffolds can be used as a carrier to target and deliver macromolecules to injured cartilage via CD44 receptors.

3.3. Micro-CT analysis

The ability of HA microscaffolds and EPO-loaded HA microscaffolds to promote chondrogenic regeneration was evaluated using an animal model. Injured cartilage specimens were treated with microscaffolds (as control), free EPO, HA microscaffolds (HA) or microscaffolds loaded with EPO (HA + EPO). After implantation for different periods of time, the synovial fluid and cartilage tissue were isolated for different analyses. The 12- and 26-week implants underwent Micro-CT imaging and

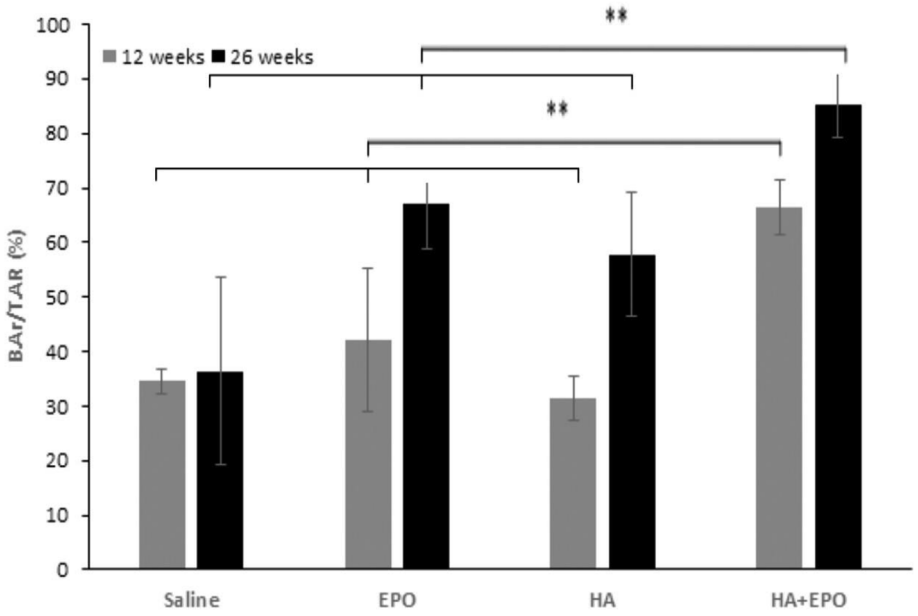

Fig. 3. Micro-CT image analysis of the rabbit cartilages 12- and 26-weeks post-surgery. Bone volume fraction (BVF) data was extracted form micro-CT images VOI. (Mean ± SD; n = 4, **p < 0.01).

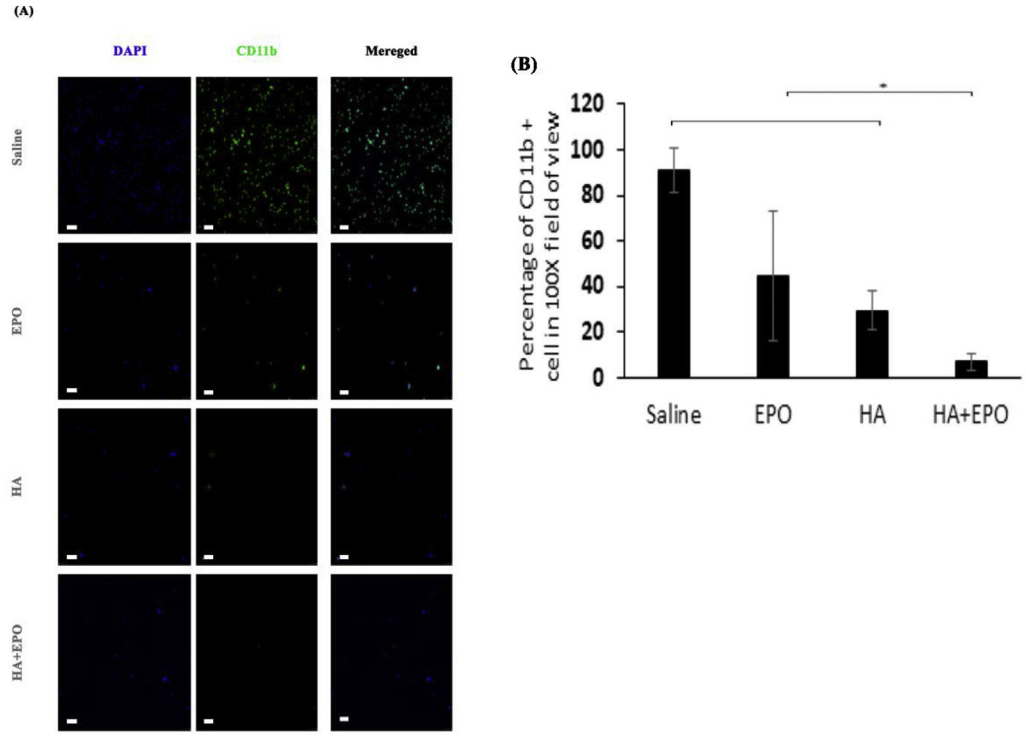

Fig. 4. The presence of CD11b + inflammatory cells in synovial fluid of treated tissues 12-week post-surgery. (A) Inflammatory cells detection migrated to the synovial fluid (scale bar 100 μm). (B) Quantification of inflammatory cells presence in the synovial fluid (Mean ± SD; n = 4, **p < 0.01).

reconstruction process (Fig. 3). The quantitative data extracted from micro-CT confirmed that, at week 12, there was no significant difference in bone volume fraction (BVF) between the EPO (42.16 ± 13.21%), HA (31.49 ± 4.14%), and saline (34.52 ± 2.15%) (Fig. 3). On the other hand, the BVF of the EPO (67.12 ± 13.21%) and HA (57.76 ± 11.42%) is significantly higher than the saline (36.34 ± 17.16%) 26 weeks post-surgery (Fig. 3). In addition, the BVF of the HA + EPO is significantly higher compared to all other groups 12 weeks (66.54 ± 5.00%) and 26 weeks (85.30 ± 6.13%) post-operatively (*p*-values < 0.01). Taken together, the micro-CT results demonstrate that the HA + EPO treatment possesses the ability to stimulate cartilage repair as early as at week 12. Such accelerated regeneration of HA + EPO treatment continues at even week 26. On the other hand, individually EPO and HA microscaffold treatment groups did not show significant healing at week 12. Both free EPO and HA microscaffold treatment groups only showed a sign of cartilage regeneration at a later time point – week 26.

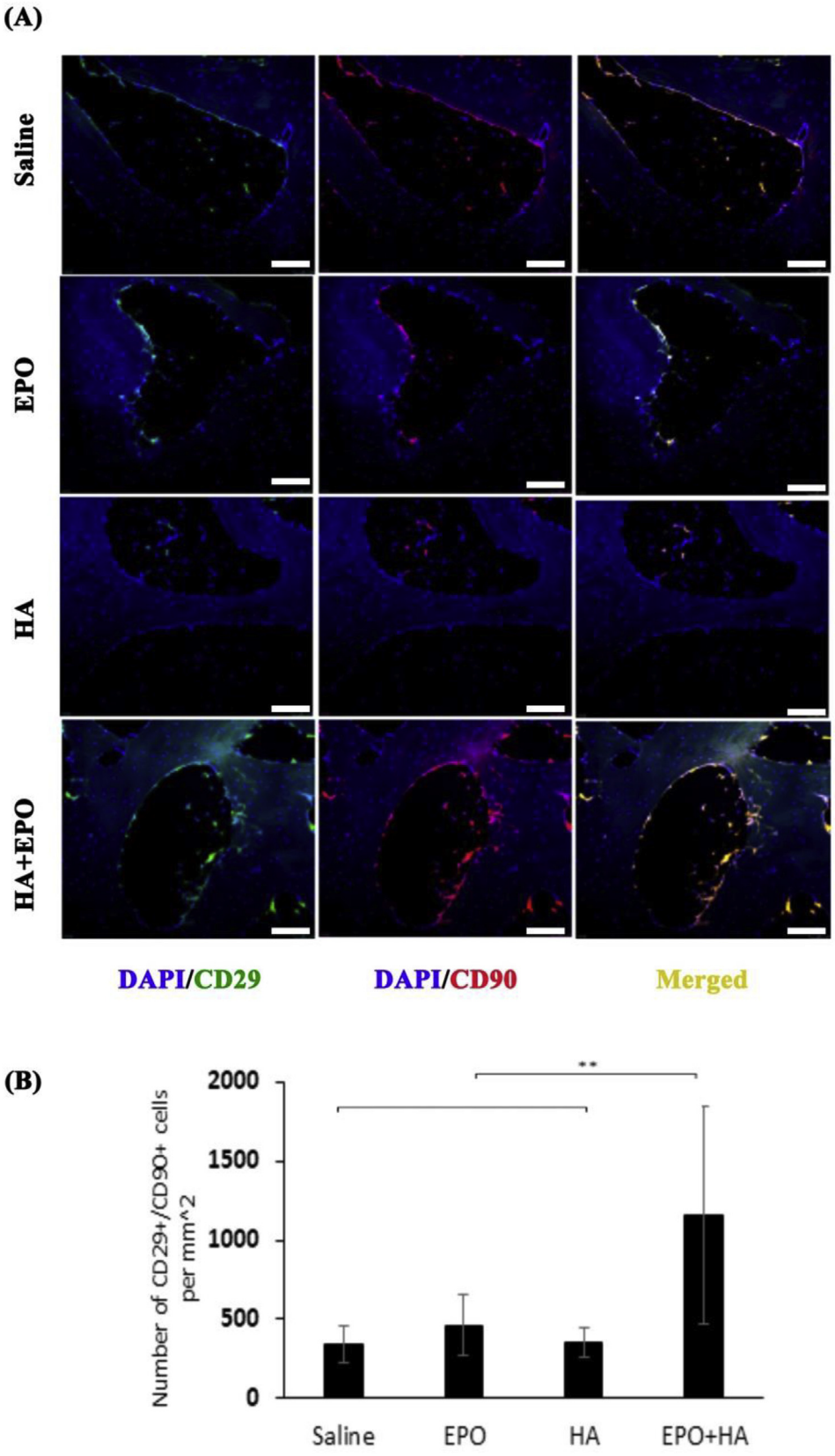

Fig. 5. Recruitment of CD29 + /CD90 + progenitor cells in variously treated tissues 12-week post-surgery. (A) Images of progenitor cells at the injury site (scale bar 100 μm). (B) Quantification of progenitor cells recruited to the injured cartilage (Mean ± SD; n = 4, **p < 0.01).

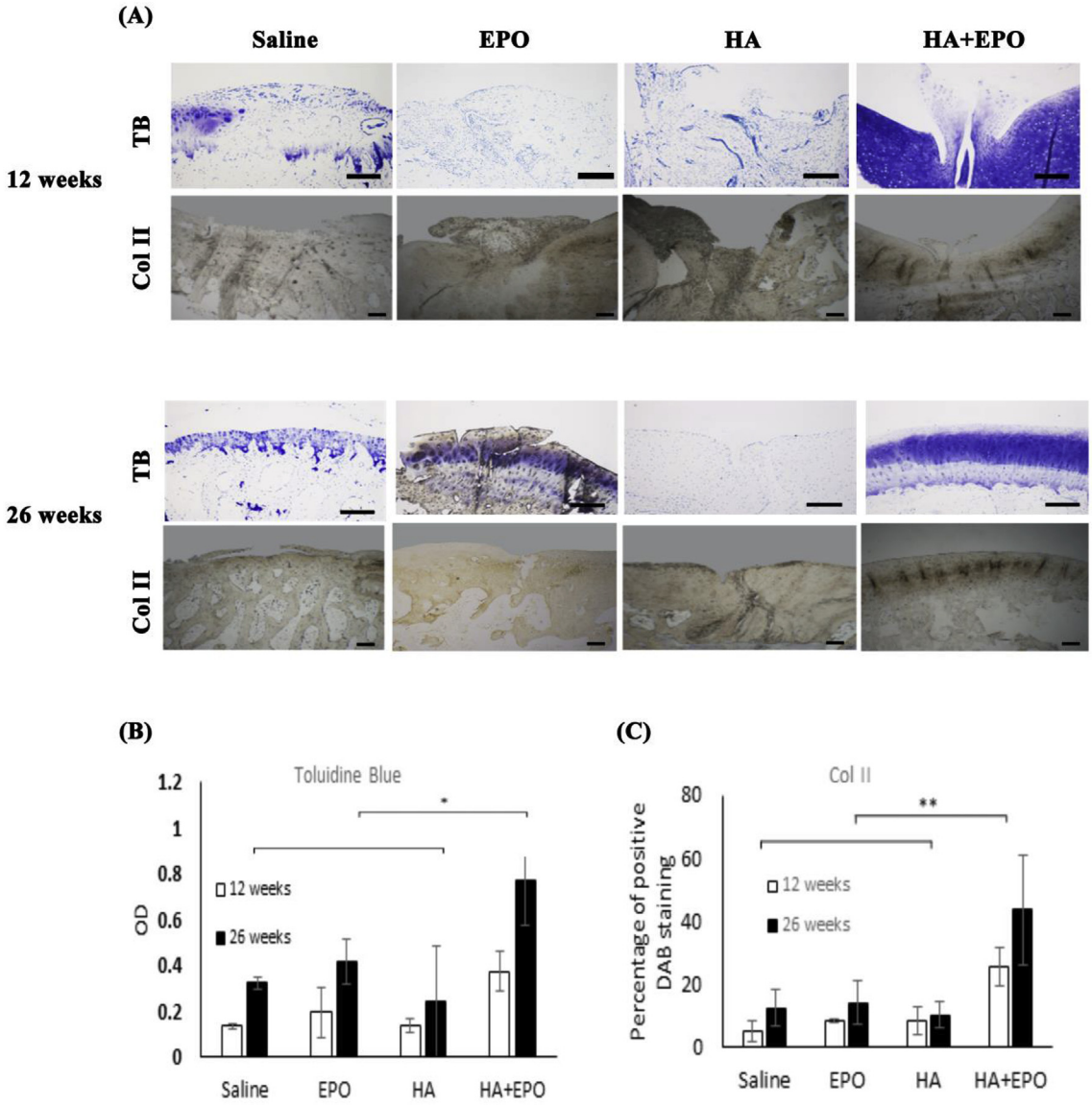

Fig. 6. Chondrogenesis evaluation of the rabbit cartilage 12- and 26-weeks post-surgery. (A) Images of tissues stained with toluidine blue (labeled as "TB") or collagen II (labeled as "Col II") (scale bar 200 μm). (B) Quantification and statistical analyses of toluidine blue and collage II stained tissue (Mean ± SD; n = 4, *p < 0.5, **p < 0.01).

3.4. Synovial cell analysis

Subsequent analyses were carried out to assess the ability of various treatments on inflammatory responses in synovial fluid. It is well established that the increasing number of inflammatory cells in the synovial fluid is an indicator of early OA [43]. As shown in Fig. 4A, among all treatment groups, HA + EPO treatment group has the lowest numbers of CD11b + inflammatory cells in the synovial fluid. Specifically, the treatment of EPO, HA, or HA + EPO reduced the inflammatory cell recruitment in synovial fluid for 45.9 ± 28.6, 29.5 ± 8.8, or 6.8 ± 3.7%, respectively (Fig. 4B). The mechanism(s) governing the reduction of inflammatory responses in the HA + EPO treatment group has yet to be determined. It is possible that such anti-inflammatory reactions may be attributed to HA's ability to bind CD44, the ligand of leukocytes [44]. HA binding may limit leukocytes' ability to interact with injured cartilage/activated macrophages and lead to their depletion from synovial fluids. In fact, it is well established that CD44, a leukocyte receptor, play an important role in inflammation [45]. Finally, EPO has been reported to have an anti-inflammatory effect as well [46].

3.5. Progenitor cell recruitment

We have hypothesized that the improved healing effect of EPO-loaded HA microscaffolds is caused by the increasing recruitment of endogenous progenitor cells to the site of cartilage injury and degeneration. To test the hypothesis, we analyzed and compared the presence of progenitor cells at the site of the injured cartilage among different groups, at week 12. Both CD29 and CD90 markers were used to identify the presence of progenitor cells in injured cartilage for primarily two reasons. First, it is well established that CD29, CD44, CD90, and CD105 are positive markers for progenitor/stem cells [34,47,48]. Second, many studies reported the increased expression of CD29 and CD90 on the MSCs [35,36]. Our results show that, as expected, there are more (~3.4 fold) $CD29^+$ (green)/CD90 (red) cells (1156 ± 683 cells/mm^2) at the site of injury than the control group (Fig. 5A and B). On the other hand, the treatments of EPO and HA microscaffolds alone did not increase progenitor cell recruitment when compared to the non-treatment control (Fig. 5A and B). These results support our overall assumption that the HA + EPO treatment enhanced the recruitment of progenitor cells to the site of injured cartilage which might lead to accelerated

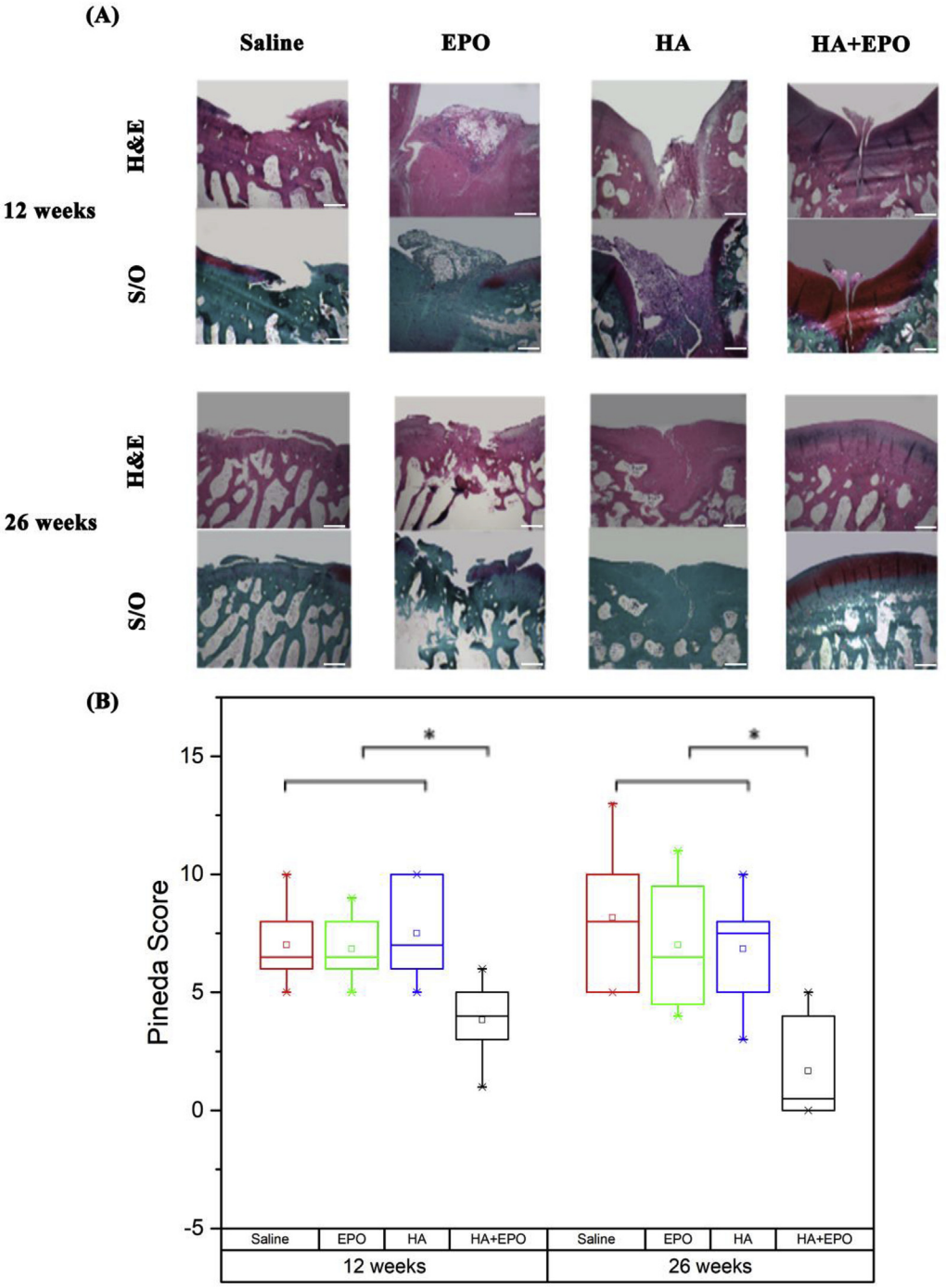

Fig. 7. Histology analysis of the defect rabbit cartilage 12- and 26-weeks post-surgery. (A) Images of H&E staining & Safranin O staining (scale bar 500 μm). (B) Pineda repair scores of the repaired cartilage based on H&E and safranin O staining of the cartilage. The lower Pineda score, the more cartilage regeneration. (Median ± interquartile range; n = 3, *p < 0.5).

cartilage regeneration.

3.6. Chondrogenesis evaluation

To assess whether the recruited progenitor cells induce chondrogenic differentiation, we investigated the expression of two major chondrogenic biomarkers (proteoglycans and collagen II) on different tissue samples using Toluidine blue and immunohistochemical staining, respectively [49]. Representative tissue images are shown in Fig. 6A. Higher glycosaminoglycan (GAG) deposition (both proteoglycans and collagen II) were seen in HA + EPO than those in controls, EPO and HA at week 12 and 26 (Fig. 6B and C). However, there was no statistically significant difference in both chondrogenic markers among the control group, HA group and EPO group (Fig. 6B and C). The overall results support that HA + EPO treatment may not only facilitate the recruitment of progenitor cells but also significantly improve chondrogenesis at the injury site as reflected by localized increased GAG and collagen II production.

3.7. Histology assessment of the repaired tissues

To evaluate the ability of HA + EPO to complete repair of the

injured cartilage, all the tissues sections were further analyzed using H& E and safranin O staining for morphological and cartilage tissue regeneration (GAG production) (Fig. 7). At week 12, the saline group had the most irregular tissue morphology as compared with other groups. The defect area in EPO and HA groups was filled with unintegrated and loose tissue while HA + EPO treatment had more highly organized tissue filled with chondrocyte-like cells (Fig. 7A). Meanwhile, the tissue section images from 26 weeks post-surgery showed that the saline and EPO treatment still had empty spaces in the place of the injury, surrounded by a poorly organized and disordered tissue. On the other hand, HA and HA + EPO treatment were shown to have regenerated a well-integrated and organized tissue within the defect sites (Fig. 7A). Specifically, HA treatment generated some fibroblast-like tissue in the place of the injury while HA + EPO treatment generated cartilage-like tissue in the defect site, integrating well with the surrounding site and providing a smooth continuous surface. Although the EPO treatment shows a high production of GAG, it was not well distributed throughout the entire repair tissue. The repaired cartilage was evaluated according to the Pineda cartilage repair score, on 4 different categories (Table 1 supplementary). The overall results show that HA + EPO had the lowest Pineda repair scores among all groups in both time points (Fig. 7B). In summary, the histology data demonstrated that, by preferentially recruited progenitor cells at the sites of injured cartilage, the HA + EPO treatment can significantly increase cartilage regeneration starting at week 12 post-surgery and achieve complete tissue recovery by 26 weeks.

4. Conclusion

In this study, a new treatment-EPO loaded HA microscaffolds were developed and investigated for their ability to stimulate and support cartilage regeneration in injured cartilage by eliciting endogenous progenitor cell response. Our *in vitro* results determined the released kinetic and bioactivity of released EPO releases from HA microscaffolds for recruiting progenitor cells. On the other hand, HA microscaffolds are found to have a high affinity for human chondrocytes and osteoarthritic tissue by interacting with their CD44 receptor. The chondrogenic property of EPO-loaded HA microscaffolds was evaluated using a rabbit microfracture defect model. The *in vivo* data showed that EPO loaded HA microscaffolds not only reduced the inflammatory cells in synovial fluid but also enhanced endogenous progenitor cell recruitment and improved the regeneration of cartilage tissue. Overall results support that EPO loaded HA microscaffolds have a great potential to be used as a treatment for regeneration of injured cartilage by inducing endogenous progenitor cell responses.

Declaration of competing interest

None.

Acknowledgment

This work was supported by a grant from Congressionally Directed Medical Research Programs, 2013 Peer Reviewed Orthopaedic Research Program, Translational Research Award (W81XWH-14-1-0459). Opinions, interpretations, conclusions, and recommendations were those of the authors and are not necessarily endorsed by the Department of Defense.

Appendix A. Supplementary data

Supplementary data to this article can be found online at https://doi.org/10.1016/j.bioactmat.2020.01.007.

References

[1] M. Favero, et al., Early knee osteoarthritis, RMD Open 1 (Suppl 1) (2015) e000062.
[2] J.C. Rivera, et al., Post-traumatic OA: Unique Implications for the Military, (2013).
[3] H. Cho, et al., Study of osteoarthritis treatment with anti-inflammatory drugs: cyclooxygenase-2 inhibitor and steroids, BioMed Res. Int. 2015 (2015) 595273, , https://doi.org/10.1155/2015/595273.
[4] I. Sekiya, et al., In vitro cartilage formation by human adult stem cells from bone marrow stroma defines the sequence of cellular and molecular events during chondrogenesis, Proc. Natl. Acad. Sci. Unit. States Am. 99 (7) (2002) 4397–4402.
[5] D. Bosnakovski, et al., Chondrogenic differentiation of bovine bone marrow mesenchymal stem cells (MSCs) in different hydrogels: influence of collagen type II extracellular matrix on MSC chondrogenesis, Biotechnol. Bioeng. 93 (6) (2006) 1152–1163.
[6] M.J. Leijs, et al., Effect of arthritic synovial fluids on the expression of immunomodulatory factors by mesenchymal stem cells: an explorative in vitro study, Front. Immunol. 3 (2012) 231.
[7] S. Suzuki, et al., Properties and usefulness of aggregates of synovial mesenchymal stem cells as a source for cartilage regeneration, Arthritis Res. Ther. 14 (3) (2012) R136.
[8] J. Lu, et al., Increased recruitment of endogenous stem cells and chondrogenic differentiation by a composite scaffold containing bone marrow homing peptide for cartilage regeneration, Theranostics 8 (18) (2018) 5039.
[9] F.-M. Chen, et al., Homing of endogenous stem/progenitor cells for in situ tissue regeneration: promises, strategies, and translational perspectives, Biomaterials 32 (12) (2011) 3189–3209.
[10] M.B. Oliveira, J.F. Mano, Polymer-based microparticles in tissue engineering and regenerative medicine, Biotechnol. Prog. 27 (4) (2011) 897–912.
[11] X. Xu, et al., Hyaluronic acid-based hydrogels: from a natural polysaccharide to complex networks, Soft Matter 8 (12) (2012) 3280–3294.
[12] M. Litwiniuk, et al., Hyaluronic acid in inflammation and tissue regeneration, Wounds 28 (3) (2016) 78–88.
[13] S.L. Hayward, C.L. Wilson, S. Kidambi, Hyaluronic acid-conjugated liposome nanoparticles for targeted delivery to CD44 overexpressing glioblastoma cells, Oncotarget 7 (23) (2016) 34158.
[14] F.-J. Zhang, et al., Expression of CD44 in articular cartilage is associated with disease severity in knee osteoarthritis, Mod. Rheumatol. 23 (6) (2013) 1186–1191.
[15] R.-H. Deng, B. Qiu, P.-H. Zhou, Chitosan/hyaluronic acid/plasmid-DNA nanoparticles encoding interleukin-1 receptor antagonist attenuate inflammation in synoviocytes induced by interleukin-1 beta, J. Mater. Sci. Mater. Med. 29 (10) (2018) 155.
[16] X. Xu, et al., Heparin-decorated, hyaluronic acid-based hydrogel particles for the controlled release of bone morphogenetic protein 2, Acta Biomater. 7 (8) (2011) 3050–3059.
[17] N. Liu, et al., Effect of erythropoietin on mesenchymal stem cell differentiation and secretion in vitro in an acute kidney injury microenvironment, Genet. Mol. Res. 12 (2013) 6477–6487.
[18] A.M. Nair, et al., The effect of erythropoietin on autologous stem cell-mediated bone regeneration, Biomaterials 34 (30) (2013) 7364–7371.
[19] C. Hidaka, et al., Acceleration of cartilage repair by genetically modified chondrocytes over expressing bone morphogenetic protein-7, J. Orthop. Res. 21 (4) (2003) 573–583.
[20] S. Li, et al., Hyaluronic acid-based optical probe for the diagnosis of human osteoarthritic cartilage, Nanotheranostics 2 (4) (2018) 347.
[21] H.Y. Yoon, et al., Tumor-targeting hyaluronic acid nanoparticles for photodynamic imaging and therapy, Biomaterials 33 (15) (2012) 3980–3989.
[22] K. Hirata, et al., Chemical synthesis and cytotoxicity of neo-glycolipids; rare sugar-glycerol-lipid compounds, Heliyon 4 (10) (2018) e00861.
[23] P.T. Thevenot, et al., The effect of incorporation of SDF-1α into PLGA scaffolds on stem cell recruitment and the inflammatory response, Biomaterials 31 (14) (2010) 3997–4008.
[24] Z. Peng, et al., Design of a portable imager for near-infrared visualization of cutaneous wounds, J. Biomed. Optic. 22 (1) (2017) 016010.
[25] S.-W. Kang, et al., Articular cartilage regeneration with microfracture and hyaluronic acid, Biotechnol. Lett. 30 (3) (2008) 435–439.
[26] E. Strauss, et al., The efficacy of intra-articular hyaluronan injection after the microfracture technique for the treatment of articular cartilage lesions, Am. J. Sports Med. 37 (4) (2009) 720–726.
[27] M.R. Clatworthy, K.G. Smith, FcγRIIb balances efficient pathogen clearance and the cytokine-mediated consequences of sepsis, J. Exp. Med. 199 (5) (2004) 717–723.
[28] X. Li, et al., Knee loading inhibits osteoclast lineage in a mouse model of osteoarthritis, Sci. Rep. 6 (2016) 24668.
[29] X.X. Shao, et al., Evaluation of a hybrid scaffold/cell construct in repair of high-load-bearing osteochondral defects in rabbits, Biomaterials 27 (7) (2006) 1071–1080.
[30] B. Grigolo, et al., Osteoarthritis treated with mesenchymal stem cells on hyaluronan-based scaffold in rabbit, Tissue Eng. C Methods 15 (4) (2009) 647–658.
[31] N. Schmitz, et al., Basic methods in histopathology of joint tissues, Osteoarthritis Cartilage 18 (2010) S113–S116.
[32] J. Shi, et al., Nanopolymers delivery of the bone morphogenetic protein-4 plasmid to mesenchymal stem cells promotes articular cartilage repair in vitro and in vivo, J. Nanomater. 2012 (2012) 2.
[33] F. Varghese, et al., IHC Profiler: an open source plugin for the quantitative evaluation and automated scoring of immunohistochemistry images of human tissue samples, PloS One 9 (5) (2014) e96801.

[34] J. Deng, et al., A silk fibroin/chitosan scaffold in combination with bone marrow-derived mesenchymal stem cells to repair cartilage defects in the rabbit knee, J. Mater. Sci. Mater. Med. 24 (8) (2013) 2037–2046.
[35] S.L. Tan, et al., Isolation, characterization and the multi-lineage differentiation potential of rabbit bone marrow-derived mesenchymal stem cells, J. Anat. 222 (4) (2013) 437–450.
[36] J. Yang, et al., Regulation of the secretion of immunoregulatory factors of mesenchymal stem cells (MSCs) by collagen-based scaffolds during chondrogenesis, Mater. Sci. Eng. C 70 (2017) 983–991.
[37] H.J. Lee, et al., Changes in surface markers of human mesenchymal stem cells during the chondrogenic differentiation and dedifferentiation processes in vitro, Arthritis Rheum.: Off. J. Am. Coll. Rheumatol. 60 (8) (2009) 2325–2332.
[38] W. Yang, et al., Targeted delivery of FGF2 to subchondral bone enhanced the repair of articular cartilage defect, Acta Biomater. 69 (2018) 170–182.
[39] D.Y. Park, et al., The degeneration of meniscus roots is accompanied by fibrocartilage formation, which may precede meniscus root tears in osteoarthritic knees, Am. J. Sports Med. 43 (12) (2015) 3034–3044.
[40] M.K. Khang, et al., Preparation of a novel injectable in situ-gelling nanoparticle with applications in controlled protein release and cancer cell entrapment, RSC Adv. 8 (60) (2018) 34625–34633.
[41] L. Wan, et al., EPO promotes bone repair through enhanced cartilaginous callus formation and angiogenesis, PloS One 9 (7) (2014) e102010.
[42] C.B. Knudson, W. Knudson, Hyaluronan and CD44: modulators of chondrocyte metabolism, Clin. Orthop. Relat. Res. 427 (2004) S152–S162.
[43] M.J. Benito, et al., Synovial tissue inflammation in early and late osteoarthritis, Ann. Rheum. Dis. 64 (9) (2005) 1263–1267.
[44] Y. Katayama, et al., CD44 is a physiological E-selectin ligand on neutrophils, J. Exp. Med. 201 (8) (2005) 1183–1189.
[45] E. Puré, C.A. Cuff, A crucial role for CD44 in inflammation, Trends Mol. Med. 7 (5) (2001) 213–221.
[46] Q. Feng, Beyond Erythropoiesis: the Anti-inflammatory Effects of Erythropoietin, Elsevier Science, 2006.
[47] C.M. Kolf, E. Cho, R.S. Tuan, Mesenchymal stromal cells: biology of adult mesenchymal stem cells: regulation of niche, self-renewal and differentiation, Arthritis Res. Ther. 9 (1) (2007) 204.
[48] S. Kern, et al., Comparative analysis of mesenchymal stem cells from bone marrow, umbilical cord blood, or adipose tissue, Stem Cell. 24 (5) (2006) 1294–1301.
[49] R. Cancedda, Cartilage and bone extracellular matrix, Curr. Pharmaceut. Des. 15 (12) (2009) 1334–1348.